Procedia Engineering

Volume 143, 2016, Pages 1108–1119

Advances in Transportation Geotechnics 3 . The 3rd International Conference on Transportation Geotechnics (ICTG 2016)

Application of Shock Mats in Rail Track Foundation Subjected to Dynamic Loads

Sinniah K. Navaratnarajah[1*], Buddhima Indraratna[1] and Sanjay Nimbalkar[1]

[1]*Centre for Geomechnaics and Railway Engineering, University of Wollongong, Australia*

skn999@uowmail.edu.au, indra@uow.edu.au, sanjayn@uow.edu.au

Abstract

Rail track substructure (ballast, subballast and subgrade) is the most essential component of the railway system in view of track stability. The ballast is the largest component of the track substructure and it is the key load-bearing stratum packed with rock aggregates underneath and around the sleepers, thereby providing structural support against dynamic stresses caused by moving trains. However under large dynamic stresses exerted by heavy haul and high speed trains, the degradation of track substructure including ballast becomes significant. This in turn affects the track stability and creates frequent maintenance, thus increasing the life cycle cost of the rail network. Therefore, mitigating degradation of the ballast layer is vital in view of track longevity. In recent years, the use of resilient soft pads (shock mats) above the ballast (i.e. Under Sleeper Pad, USP) and below the ballast (i.e. Under Ballast Mat, UBM) has become a common practice. Many countries, including Australia have adopted the use of resilient pads in the rail track foundation. Currently, the studies on resilient mats are mostly limited to the reduction of vibration and noise. There is a lack of proper assessment of the geotechnical behavior of ballast when used along with shock mats. This paper provides an assessment of the triaxial behavior of the track substructure with and without shock mats under dynamic loading condition. A numerical model was developed based on the modified stress-dilatancy approach to capture the stress-strain and volume change behavior of ballast during impact loading. Model predictions are compared with laboratory results. It was found that the shock mats provide significant advantages in terms of reduced particle breakage and enhanced track stability.

Keywords: ballast; cyclic load; impact load; shock mat; deformation; degradation

1 Introduction

Improving the railroad stability to operate freight and passenger services has become one of the key challenges globally. Railway industries are placing greater emphasis on implementing high train speed corridors and heavier freight operations to achieve efficient and cost-effective services. Increasing train speed and axle load causes high undue stresses transferred to the ballast and

* Corresponding author

Selection and peer-review under responsibility of the Scientific Programme Committee of ICTG 2016

doi:10.1016/j.proeng.2016.06.152

underlying formation. Ballast degradation is a major factor affecting track longevity and stability. The adoption of various forms of artificial shock mats such as Under Sleeper Pad (USP) and Under Ballast Mat (UBM) as means of reducing ballast plastic deformation and degradation has become increasingly popular in recent years (Bolmsvik, 2005; Esveld, 2001; Marschnig and Veit, 2011; Schneider et al., 2011). These resilient pads avoids a hard interface with ballast to the sleeper or underlying formations, allowing the aggregates to bed into the relatively softer pad and thereby increasing the contact surface area of the ballast and reducing ballast stresses. However, studies conducted to analyse the application of shock mats in minimizing ballast degradation are limited. This paper presents a review of recently published work performed using the state-of-the-art large-scale testing apparatus at the University of Wollongong to evaluate the performance of shock mats in reducing the ballast deformation and degradation.

2 Large Scale Dynamic Load Testing

To assess the role of shock mats in reducing the ballast deformation and degradation, a series of large scale impact and cyclic load tests were conducted at the University of Wollongong, New South Wales (NSW), Australia. Impact loads were simulated using a high-capacity drop-weight impact testing equipment and cyclic loading tests were conducted using the state-of-the-art large-scale process simulation prismoidal triaxial apparatus (PSPTA). The ballast material commonly used in NSW rail track was used for the laboratory testing.

2.1 Test Materials and Specifications

The materials used in this study are the fresh ballast, subballast, subgrade and shock mats. The fresh ballast tested is latite (volcanic) basalt, a common igneous rock that can be found along the south coast of NSW, and obtained from Bombo quarry, near Wollongong, Australia. The ballast samples were prepared in accordance with current Australian practices (AS 2758.7, 2015). The laboratory samples were cleaned by water to remove any dust and clay adhering to the surface of the aggregates and dried before screening through selected sieve sizes and then mixed in desired proportions to obtain the required particle size distribution. Sand and steel plates were used to simulate comparatively weak and hard subgrade conditions, respectively in the impact load testing. The subballast used for cyclic load testing was also obtained from Bombo quarry, NSW. The particle size distribution and the grain size characteristics of materials are shown in Figure 1.

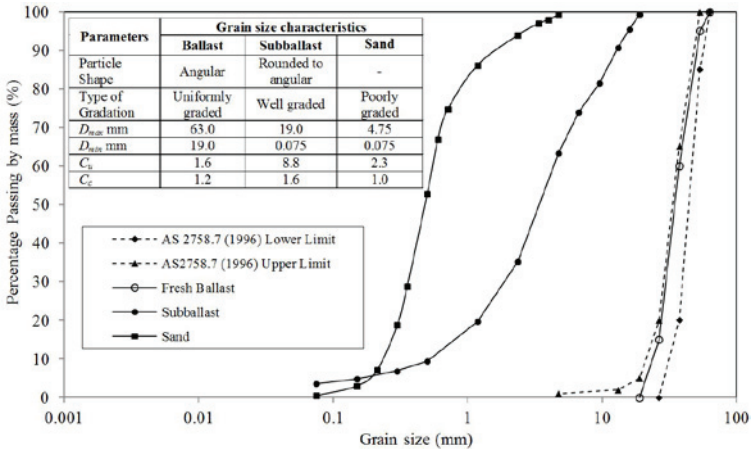

Figure 1: Particle size distribution and grain size characteristics

The mechanical properties of the shock mats used in this study are shown in Table 1. The recycled rubber shock mat used for impact load testing was 10 mm thick, and was made of recycled rubber granulates encapsulated within a polyurethane elastomer compound. The 10 mm thick elastoplastic USP used for cyclic load testing was made of polyurethane, and this rubber pad was glued to the bottom face of the concrete sleeper.

Shock Mat for Impact Load Test		**Shock Mat for Cyclic Load Test**	
Thickness	10 mm	Thickness	10 mm
Weight	9.2 kg/m^2	Weight	4.2 kg/m^2
Bedding Modulus	0.20 N/mm^3	Bedding Modulus	0.22 N/mm^3

Table 1: Mechanical Properties of Shock Mats

2.2 Impact Load Testing

Wheel-rail irregularities and variation in track foundation conditions causes the train wheels to impact on to the rail and thereby causing a forced vibration of high frequencies (Anastasopoulos et al., 2009; Bian et al., 2013; Indraratna et al., 2014b; Indraratna et al., 2012; Kaewunruen and Remennikov, 2007; Nielsen and Johansson, 2000). These impact forces cause accelerated ballast breakage. At a bridge approach, road crossing or track transition zone where the foundations stiffness changes from relatively weak to hard or vice versa, high impact forces are generated, usually resulting in track degradation (Indraratna et al., 2014c; Li and Davis, 2005). In this study, typical impact dynamic stresses in the range of 400-600 kPa caused by wheel flat and dipped rail at the top of ballast layer (Indraratna et al., 2010; Jenkins et al., 1974; Steffens and Murray, 2005) were simulated using a high capacity drop weight impact machine.

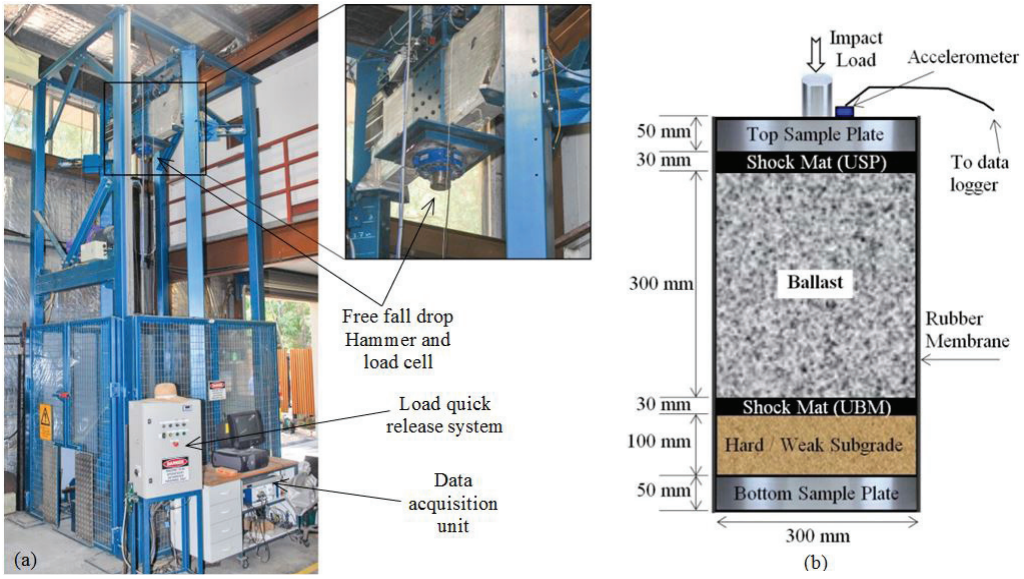

Figure 2: High capacity drop weight impact apparatus; and (b) Schematic diagram of impact test sample

The impact machine shown in Figure 2(a) consists of a 592 kg weight free fall drop hammer and it can be dropped from a maximum height of 6 m measured above the base of the strong concrete floor. The hammer can be hoisted mechanically to the predetermined height which corresponds to the required impact load magnitude. The hammer is then dropped through guided roller on vertical column to the test sample (see schematic of test sample in Figure 2b) placed in the concrete floor. The

impact load was measured by a load cell (1,200 kN maximum capacity) mounted at the bottom of the hammer and recorded in the data acquisition unit. Ballast deformation and transient acceleration of the impact loads were captured by a piezoelectric accelerometer (capacity of 10,000g where g is gravitational acceleration) connected at the top of the sample load plate. Axial and lateral strains are determined in the experiment by taking linear measurements of specimen height and circumference. These are residual strains and hence were measured during the interval between applications of successive blows.

A ballast thickness of 300 mm is found to be more realistic in simulating site condition as per the previous study on ballast material conducted on large scale triaxial testing by Brown et al. (2007) and Indraratna et al. (2007). The ballast aggregates were compacted in several layers by using a rubber padded hammer to a typical field density (approximately 1560 kg/m^3) for heavy haul tracks. The low lateral confining pressure for the ballast was provided by placing a cylindrical rubber membrane around the specimen. The 7 mm thickness rubber membrane used was capable of prevent piercing or cutting the membrane by sharp corners of ballast particles. Two types of base condition, (i) relatively weak base represented by a 100 mm thick sand layer vibro-compacted to a density of 1620 kg/m^3 and placed under the ballast bed, and (ii) hard base condition represented by a rigid steel plate of thickness 50 mm were used. This hard base condition is represented by the tracks running on steel or concrete bridge deck or track foundation located on hard bed rock terrains. Three layers of rubber pads making a total thickness of 30 mm were used at the top, bottom and both at the top and bottom of the ballast layer (see Figure 2b) and the results were compared with that of sample tested without shock mat.

The impact loading was repeated for 10 times during the testing. It was found that the strain due to impact loading was attenuated after certain number of blows (typically 8 or 9 blows). Automatic triggering of impact loading signal was enabled and data at sampling frequency of 50 kHz was collected by the data acquisition unit. To remove the noise in the data, the raw impact load-time history data were digitally filtered using low-pass fourth order Butterworth filter with a cut-off frequency of 2 kHz. Ballast deformations and transient acceleration of the impact load data were recorded by a data acquisition unit via a piezoelectric accelerometer connected at the top of the sample plate.

2.3 Cyclic Load Testing

The repeated cyclic loading from moving wheel on a rail track causes progressive deformation and degradation of ballast particles. This type of dynamic loading were simulated by the process simulation prismoidal triaxial apparatus (PSPTA) shown in Figure 3. This apparatus correctly simulates realistic stress and boundary conditions found in ballasted track. In a real rail track, the lateral movement of the ballast is not fully restrained, particularly in the direction perpendicular to the rail (Indraratna et al., 2001). Therefore, the four vertical walls of the test chamber were built to allow free movement under applied cyclic loading. In this study, only two walls (perpendicular to the rail) were allowed to move under low confinement, and the other two walls were locked in position to simulate a typical straight track (longitudinal deformation parallel to rail is negligible). The size of the cubical triaxial chamber shown in Figure 3 is 800 mm long, 600 mm wide and 600 mm high.

A ballast sample of 300 mm in thickness was placed on top the 150 mm compacted subballast layer in three equal 100 mm layers, and then compacted by a rubber padded vibratory hammer to a typical field density of approximately 1560 kg/m^3. The rail-sleeper assembly was placed on top of compacted ballast, and the space around the concrete sleeper was filled with 150 mm thickness compacted crib ballast. The cyclic loading used were equivalent to a 25 ton axle load with a frequency of 15 Hz; this simulated a train travelling at about 110 km/h (Indraratna et al., 2015). The corresponding cyclic loading is a sinusoidal wave form with a mean stress of 195 kPa and amplitude of 165 kPa at the top of ballast layer. Lateral confinement was applied through movable vertical walls that simulated a low confining stress of 10 kPa. The longitudinal directions of the walls were locked in position to ensure plane strain conditions, while the pressure exerted on the wall was measured.

Electronic potentiometers and settlement plates were used to measure the deformation of the ballast layer. The vertical and lateral load and associated deformation were recorded by data loggers connected to computers. Two tests were performed one with inclusion of USP and the other without the USP. A total of 500,000 load cycles were applied for each cyclic load test.

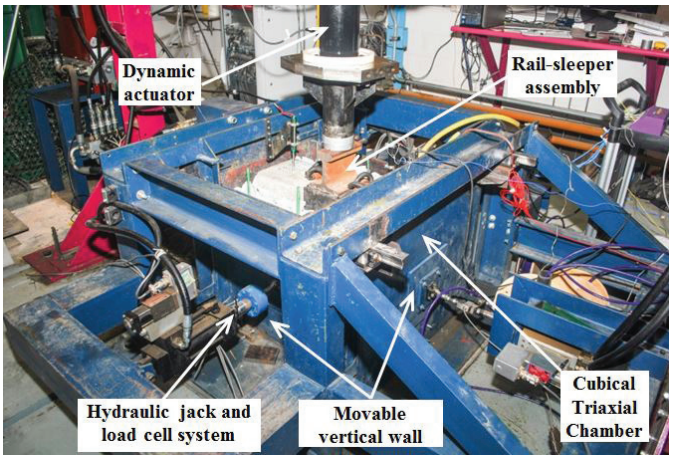

Figure 3: Process simulation prismoidal triaxial apparatus (PSPTA)

3 Numerical Analysis

The dynamic response of a layered system attributed to transient impact load was analyzed by a 2-dimentional (2D) axisymmetric finite element (FE) analysis under dynamic conditions using PLAXIS (PLAXIS 2D: Ver. 8.6). The impact test sample of this study was modeled as an elasto-plastic model of a composite layered system including ballast, shock mat, and base. The main features of this dynamic FE analysis are the introduction of modified stress-dilatancy relationship to capture the particle degradation and incorporation of material damping for various track materials tested. All layers were modeled using 15-node cubic strain elements which provide a fourth order interpolation for displacements. Interface elements were used to model the frictional behaviour between various layers and were simulated by 5-node, zero-thickness line elements. The numerical integration by the Gaussian scheme involves 12 Gauss points. The axisymmetric impact sample model simulated in finite element discretization using PLAXIS 2D is shown in Figure 4. The digitally filtered transient impact load-time histories obtained from the laboratory impact testing were used for the dynamic FE analysis. The following boundary conditions were adopted for the analysis. The axis of symmetry (left axis) and bottom boundaries were restrained in lateral and vertical directions, respectively. The top and right boundaries were free to move. The node at the left bottom corner of the mesh was restrained in both vertical and horizontal directions (pinned support - standard fixity). The right and bottom boundaries were considered absorbent boundaries. Lateral distributed loads were applied to the right boundary to represent the confining effects of thick rubber membrane (Henkel and Gilbert, 1952). Isotropic Hardening Soil model (Schanz et al., 1999) was used for ballast layer. The mobilized friction angle ϕ'_m and the mobilized dilatancy angle ψ_m (Nimbalkar et al., 2012) used are defined in Equations (1) and (2), respectively. Classical Mohr-Coulomb elastic-perfectly-plastic model was used for the sand (weak base). Steel plate (hard base) and shock mats were modelled as linear elastic. The constitutive model parameters obtained from the available laboratory test results are shown in Table 2. The other terms in the Equations (1) and (2) and terms in Table 2 are explained elsewhere (Nimbalkar et al., 2012).

$$\sin\varphi'_m = \frac{q}{q+2\sigma'_3} \tag{1}$$

$$\sin\psi_m = \frac{\left(\sin\varphi'_m - \sin\varphi'_{cv}\right) - \left\{\dfrac{\kappa\left(dBBI\right)\left(1-\sin\varphi'_m\right)}{2\sigma'_3 d\varepsilon_1^p\left(1+\tan^2\varphi'_{cv}\right)}\right\}}{\left(1-\sin\varphi'_m\ \sin\varphi'_{cv}\right) - \left\{\dfrac{\kappa\left(dBBI\right)\left(1-\sin\varphi'_m\right)}{2\sigma'_3 d\varepsilon_1^p\left(1+\tan^2\varphi'_{cv}\right)}\right\}} \tag{2}$$

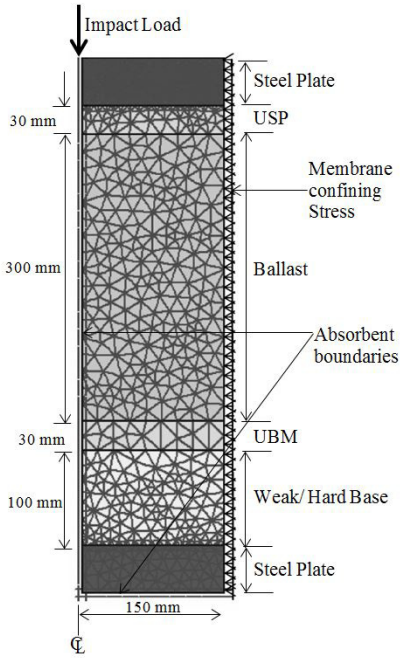

Figure 4: Finite element discretization of impact load test sample (sourced from Nimbalkar et al., 2012)

Hardening soil model for ballast	Hard Base				Weak Base				Mohr-Coulomb elasto-plastic model for sand
	Sample 1	Sample 2	Sample 3	Sample 4	Sample 5	Sample 6	Sample 7	Sample 8	$E = 45\,MPa$, $\nu = 0.33$, $c' = 0$, $\varphi' = 24^o\ and\ \ \psi = 0$
E_{50}^{ref} (MPa)	11.04	12.13	12.08	13.12	12.43	14.12	12.92	15.10	
E_{oed}^{ref} (MPa)	11.04	12.13	12.08	13.12	12.43	14.12	12.92	15.10	
E_{ur}^{ref} (MPa)	10.20	9.21	14.52	12.09	12.53	14.00	13.08	14.80	Linear elastic model for steel base $E = 210\,GPa, \nu = 0.15$ $\gamma = 77\,kN/m^3$
ϕ'_p (degrees)	73.34	73.46	73.37	73.60	74.81	75.18	75.00	75.83	
ψ (degrees)	21.27	20.76	20.08	16.15	18.20	17.14	17.82	14.58	
P_{ref} (kN/m^2)	19.70	17.24	15.14	12.67	10.65	7.88	8.95	6.06	Linear elastic model for Shock Mat $E = 6.12\ MPa$ $\nu = 0.48$ $\gamma = 12.04\,kN/m^3$
$\left(dBBI/d\varepsilon_1^p\right)_f$	0.81	0.79	0.78	0.68	0.73	0.71	0.61	0.47	
κ	882.44	835.37	738.78	728.54	664.45	573.63	703.36	674.72	
$\left(dE_B/d\varepsilon_1^p\right)_f$ (kNm/m^3)	714.78	659.94	576.25	495.41	485.05	409.41	429.05	317.12	

Table 2: Parameters used for the numerical analysis (data sourced from Nimbalkar et al., 2012)

4 Results and Discussion

A total of 8 impact load tests were conducted with varying two different base conditions (weak and hard bases) and by placing the shock mats at the top and/or bottom and the results were compared with that of without the shock mat condition. Two cyclic load tests were performed one with the under sleeper pad and the other without any shock mats. A numerical analysis was performed for impact load testing by selecting the cases (i) without any shock mats and (ii) shock mats placed at the top and bottom of the ballast layer. The laboratory findings and the finite element predictions are discussed as follows.

4.1 Axial and Lateral Strain Responses

Axial and lateral strains were calculated from the deformation data collected during impact and cyclic loading tests. The variation of axial and lateral strains with and without shock mats condition for weak and hard base conditions of the impact load tests are shown in Figures 5(a) and (b), respectively. Rapid increases of strains were observed at the initial impact blows and subsequently stabilized after around 8 impact blows. This is due to the rearrangement and corner breakage of ballast particles at the initial stage of loading and gradually diminishing thereafter. Both axial and lateral strains were higher for the ballast without shock mat, and they decreased in the order of 10-25% when introducing the shock mats either at the top or bottom of the ballast layer. When providing the shock mats at both top and bottom it works well in reducing the ballast strains and the observed strain decrement were in the order of 30-50%. The plastic strains were more pronounced for the hard subgrade compared to weak base.

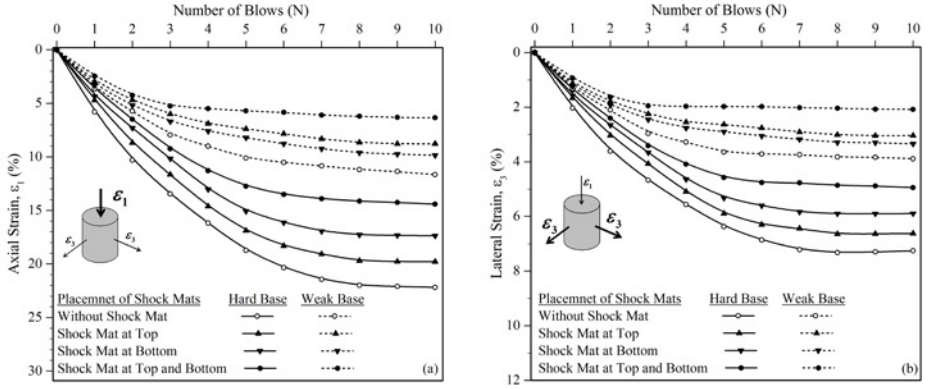

Figure 5: (a) axial; and (b) lateral strain responses from impact load test (data sourced from Nimbalkar et al., 2012)

The axial and lateral strain response of the ballast under cyclic loading with and without USP were calculated from axial and lateral displacement of the ballast measured at selected number of load cycles (e.g. N = 100, 500, 1000, 5000, 10000, etc.) and are shown in Figures 6(a) and (b), respectively. It is evident from the test results, the axial strain was reduced by about 30% by the use of USP and that of lateral strain reduction was about 10%. In both tests, the ballast deformation was rapid up to around 10,000 load cycles due to the initial densification of ballast and further packing after corner breakage of sharp angular aggregates. Once the ballast mass stabilized (after 10,000 load cycles), the rate of ballast strain decreased with the increasing number of load cycles.

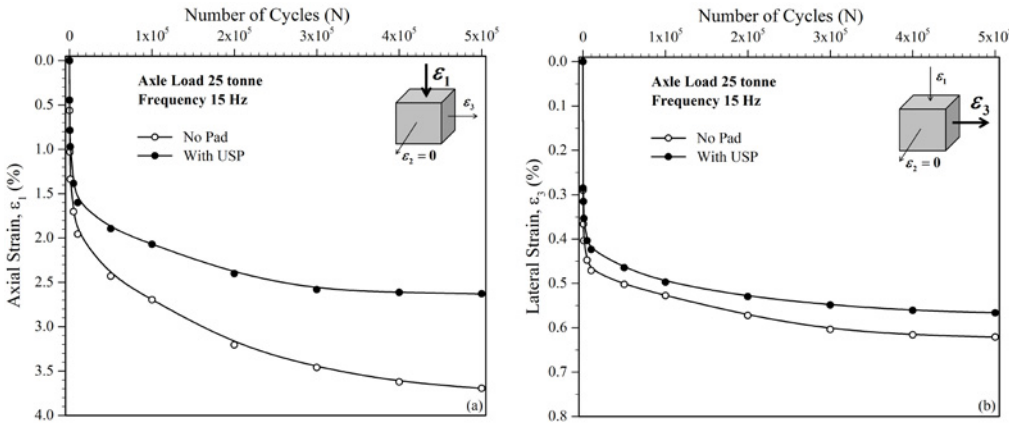

Figure 6: (a) axial; and (b) lateral strain responses from cyclic load test (data sourced from Indraratna et al., 2014a)

Figures 7(a) and (b) show the FE model prediction of the axial and lateral strain using the impact pulse data obtained in the laboratory impact testing. The strain values are compared with laboratory measured data for the case when shock mats placed at both top and bottom condition to that of without shock mat condition. The FE analysis was able to predict the strain hardening behaviour of ballast under repeated impact load and closely captured the plastic yielding of the ballast, which was influenced by the amount of viscous damping of the ballast material.

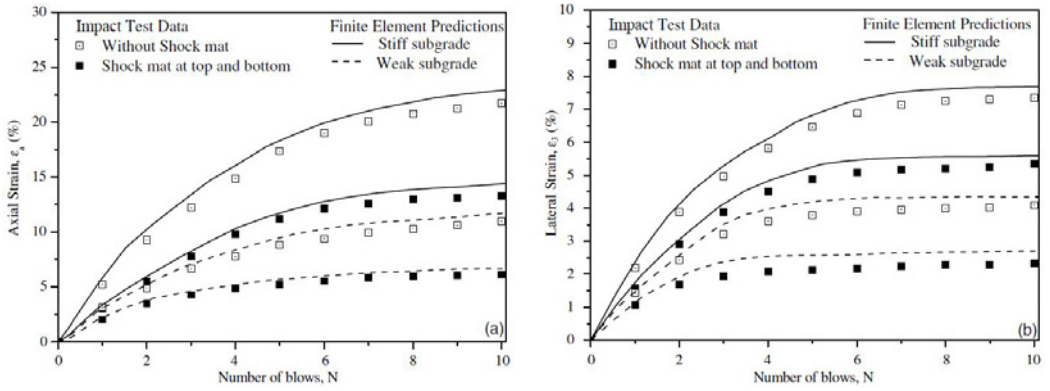

Figure 7: Numerical analysis prediction with test results: (a) axial strain; and (b) lateral strain (data sourced from Nimbalkar et al., 2012)

4.2 Ballast Degradation

Ballast degradation takes place under impact and repetitive cyclic loading. Initially, breakage of corners of the angular ballast at the inter-particle contacts takes place, followed by complete fracture across the body of the particles depending on the strength of the parent rock and the level of load increment. This breakage of ballast particles contributes to increased axial and lateral strains and causes differential track settlement. In this study, the ballast degradation was quantified by using ballast breakage index method proposed earlier by Indraratna et al. (2005). To quantify the particle breakage in this method, particle size analysis was performed before and after the tests.

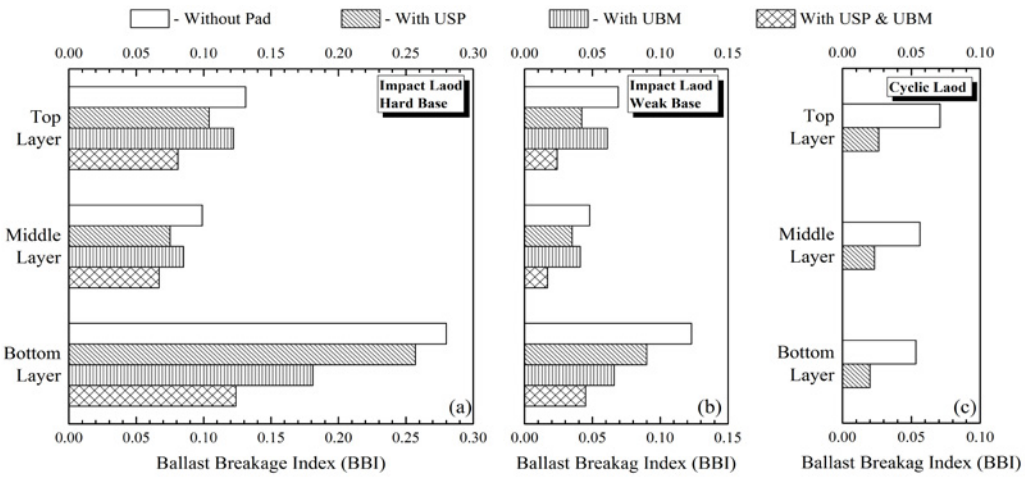

Figure 8: Ballast breakage index (BBI): (a) Impact load (hard base); (b) Impact load (weak base); and (c) cyclic load (data sourced from Indraratna et al., 2014a; Nimbalkar et al., 2012)

The BBI values for top, middle and bottom layers of ballast samples are shown in Figures 8 (a), (b) and (c) for Impact load (hard base), impact load (weak base) and cyclic load tests, respectively. Both impact and cyclic load test results show that the use of shock mats significantly reduces the particle degradation. As expected the BBI is relatively high for hard base condition compared to weak base in impact testing. Also, the BBI is minimum when the shock mats were placed both at the top and bottom of ballast layer. However, depending on the stiffness of shock mat materials, placing both USP and UBM will introduce extra deflection at the rail head level which can increase the bending stress within the rail and accelerate rail fatigue cracking. Therefore selection of shock mat with appropriate stiffness is crucial.

The cyclic test also shows the same trend as impact test on reducing degradation behavior, in that the use of under sleeper pad reducing repeated cyclic loading induced ballast breakage. It is also evident from the BBI values that ballast degradation is considerably high caused by the impact stresses than cyclic stresses.

5 Reduction of Life Cycle Cost (LCC)

Over the past 5 years, Australian rail industries have invested more than a billion dollars per year on rail transport (BITRE, 2014), a major proportion of which have been spent on the geotechnical related problems of substructure, including the ballast layer (Indraratna et al., 2002; Ionescu et al., 1998). For instance, track maintenance cost is estimated to exceed about 15 million dollars per annum in the state of New South Wales alone only for ballast related maintenance (Hussaini et al., 2012). This is primarily attributed to lack of proper attention given to the track substructure (ballast, subballast and subgrade) compared to the superstructure (rails, sleepers and fasteners).

USPs increase the load distribution areas between the sleeper and ballast since the elastic layer attached under the sleeper enables an embedding of ballast aggregates to the sleeper consequently reduces the ballast pressure. Thus reduces the cost for maintenance with a simultaneously moderate capital expenditure. The life cycle cost (LCC) analysis on Austrian railway (Marschnig and Veit, 2011; Schilder, 2013) showed that the installation of padded sleepers significantly reduced the three main cost components (depreciation, operational hindrance and maintenance) as shown in Figure 9 and subsequently reduced the total average annual cost for the track. About 20% average annual costs

was reduced by using USP at track turnout sections. In summary, the use of USP in the track is a major step towards cost efficient and sustainable ballasted track.

Soft padded concrete sleepers reduce the ballast wear and extend the intervals between two tamping cycle by at least 2 and thereby increase the service life of the ballast (Marschnig and Veit, 2011). The passenger comfort also increases by insertion of the soft padded sleepers. In addition due to the stiffness adjusting nature of USP, it can be used in locations such as transition from bridges or tunnels to open track and vice versa where the stiffness of the track changes abruptly. Reducing vibration and noise on specific areas such as tracks on tunnels or urban areas are another benefits.

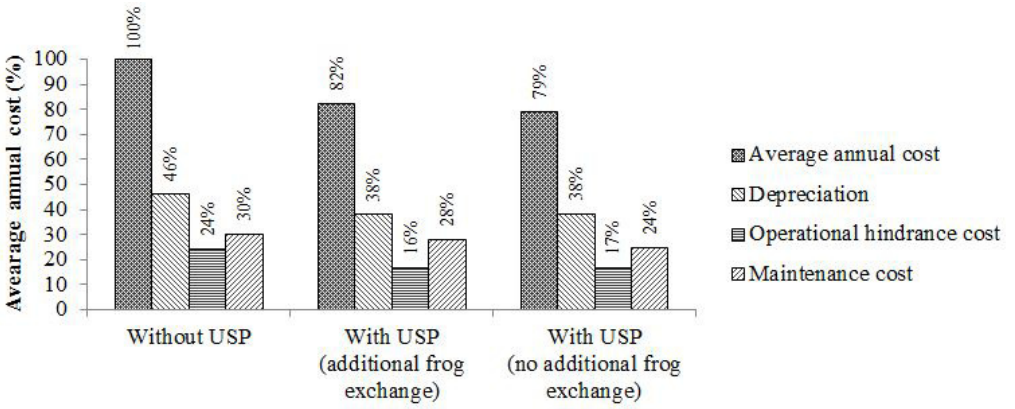

Figure 9: Life Cycle Cost (LCC) reduction by USP in turnouts (data sourced from Schilder, 2013)

6 Conclusions

The application of shock mats in rail track foundation under dynamic loads was studied through laboratory experiments and numerical models. The impact load causes accelerated ballast deformation and degradation was confirmed by experiment and numerical model data. The finite element model analysis was capable of predicting strain responses measured for ballast under impact load with and without shock mats. Two base conditions tested in this study confirm that the hard foundation (subgrade) conditions cause comparatively higher ballast deformation and degradation than a weaker base. The inclusion of shock mats at the top and/or bottom of the ballast considerably reduces the ballast deformation and degradation.

The large-scale cyclic load test with the inclusion of under sleeper pad assured that the ballast deformation could be reduced significantly. The test results also confirmed that the ballast breakage was reduced by the use of USP. It is evident from this study that by placing shock mats, loads on the ballast bed can be distributed more homogeneously with the sleepers and base under the ballast and thereby improving the track stability. This minimized degradation by shock mats leads to reduced number of maintenance operations leads to life cycle cost savings for track owners.

The selection of shock mat with appropriate stiffness and damping properties is crucial in view of their effectiveness in deformation control. The intended functions of shock mat can also be governed by its thickness and material type such as synthetic pads, recycled rubber tyre, rubber granulates etc. In view of these, further tests are necessary for comprehensive assessment of shock mats. Some of these aspects are currently under investigation at the University of Wollongong.

Acknowledgements

The authors wish to thank the Australian Research Council (ARC) for its financial support. The assistance provided by senior technical officers, Alan Grant, Cameron Neilson, Ritchie Mclean and Ian Bridge are also much appreciated. A significant portion of the contents have been reproduced with kind permission from the Journal of Geotechnical and Geoenvironmental Engineering ASCE and Australian Geomechanics Journal.

References

Anastasopoulos, I., Alfi, S., Gazetas, G., Bruni, S., & Van Leuven, A. (2009). Numerical and Experimental Assessment of Advanced Concepts to Reduce Noise and Vibration on Urban Railway Turnouts. *Journal of Transportation Engineering, 135*(5), 279-287.

Bian, J., Gu, Y., & Murray, M. H. (2013). A dynamic wheel–rail impact analysis of railway track under wheel flat by finite element analysis. *Vehicle System Dynamics, 51*(6), 784-797.

BITRE. (2014). *Infrastructure, transport and productivity*. Canberra ACT, Australia.

Bolmsvik, R. (2005). *Influence of USP on track response–a literature survey*. Abetong Teknik ABVäxjö, Sweden.

Brown, S. F., Kwan, J., & Thom, N. H. (2007). Identifying the key parameters that influence geogrid reinforcement of railway ballast. *Geotextiles and Geomembranes, 25*(6), 326-335.

Esveld, C. (2001). *Modern railway track* (2nd ed.). MRT-Production, The Netherlands.

Henkel, D. J., & Gilbert, G. D. (1952). The Effect Measured of the Rubber Membrane on the Triaxial Compression Strength of Clay Samples. *Géotechnique, 3*, 20-29.

Hussaini, S. K. K., Indraratna, B., & Vinod, J. (2012). *Performance of geosynthetically-reinforced rail ballast in direct shear conditions*. 11th Australia - New Zealand Conference on Geomechanics: Ground Engineering in a Changing World.

Indraratna, B., Biabani, M., & Nimbalkar, S. (2015). Behavior of Geocell-Reinforced Subballast Subjected to Cyclic Loading in Plane-Strain Condition. *Journal of Geotechnical and Geoenvironmental Engineering, 141*(1), 1-16.

Indraratna, B., Lackenby, J., & Christie, D. (2005). Effect of confining pressure on the degradation of ballast under cyclic loading. *Géotechnique, 55*(4), 325-328.

Indraratna, B., Navaratnarajah, S. K., Nimbalkar, S., & Rujikiatkamjorn, C. (2014a). Use of shock mats for enhanced stability of railroad track foundation. *Australian Geomechanics Journal, Special Edition: ARC Centre of Excellence for Geotechnical Science and Engineering, 49*(4), 101-111.

Indraratna, B., Nimbalkar, S., Christie, D., Rujikiatkamjorn, C., & Vinod, J. (2010). Field Assessment of the Performance of a Ballasted Rail Track with and without Geosynthetics. *Journal of Geotechnical and Geoenvironmental Engineering, 136*(7), 907-917.

Indraratna, B., Nimbalkar, S., Navaratnarajah, S. K., Rujikiatkamjorn, C., & Neville, T. (2014b). Use of shock mats for mitigating degradation of railroad ballast. *Sri Lankan geotechnical journal - Special issue on ground improvement, 6*(1), 32-41.

Indraratna, B., Nimbalkar, S., & Neville, T. (2014c). Performance assessment of reinforced ballasted rail track. *Proceedings of the ICE-Ground Improvement, 167*(1), 24-34.

Indraratna, B., Nimbalkar, S., & Rujikiatkamjorn, C. (2012). *Performance evaluation of shock mats and synthetic grids in the improvement of rail ballast.* 2nd Int. Conference on Transportation Geotechnics (ICTG), Sapporo, Japan.

Indraratna, B., Salim, W., & Christie, D. (2002). *Improvement of recycled ballast using geosynthetics.* Proc. 7th International Conference on Geosynthetics, Nice, France.

Indraratna, B., Salim, W., Ionescu, D., & Christie, D. (2001). *Stress-strain and degradation behaviour of railway ballast under static and dynamic loading, based on large-scale triaxial testing.* Proc. 15th Int. Conference on Soil Mechanics and Getechnical Engineering, Istanbul.

Indraratna, B., Shahin, M. A., & Salim, W. (2007). Stabilisation of granular media and formation soil using geosynthetics with special reference to railway engineering. *Journal of Ground Improvement, 11*, 27-43.

Ionescu, D., Indraratna, B., & Christie, H. D. (1998, 9-12 November). *Behaviour of railway ballast under dynamic loads.* Proc. 13th South East Asian Geotechnical Conference, Taipei.

Jenkins, H. M., Stephenson, J. E., Clayton, G. A., Moorland, J. W., & Lyon, D. (1974). The effect of track and vehicle parameters on wheel/rail vertical dynamic forces. *Railway Engineering Journal, 3*(1), 2-16.

Kaewunruen, S., & Remennikov, A. M. (2007). *Response and Prediction of Dymanic Characteristics of Worn Rail Pads Under Static Preloads*. 14th International Congress on Sound and Vibration.

Li, D., & Davis, D. (2005). Transition of Railroad Bridge Approaches. *Journal of Geotechnical and Geoenvironmental Engineering, 131*(11), 1392-1398.

Marschnig, S., & Veit, P. (2011). Making a Case For Under-Sleeper Pads. *International Railway Journal, 51*(1), 27-29.

Nielsen, J. C. O., & Johansson, A. (2000). Out-of-round railway wheels - a literature survey. *Proceedings of the Institution of Mechanical Engineers Part F-Journal of Rail and Rapid Transit, 214*(2), 79-91.

Nimbalkar, S., Indraratna, B., Dash, S., & Christie, D. (2012). Improved Performance of Railway Ballast under Impact Loads Using Shock Mats. *Journal of Geotechnical and Geoenvironmental Engineering, 138*(3), 281-294.

Schanz, T., Vermeer, P. A., & Bonnier, P. G. (1999). *The hardening soil model: Formulation and verification.* Beyond 2000 in Computational Geotechnics, Balkema, Rotterdam.

Schilder, R. (2013). *Track innovations by Austrian railways.* Proceedings of the AREMA 2013 annual conference, Indianapolis, IN.

Schneider, P., Bolmsvik, R., & Nielsen, J. C. O. (2011). In situ performance of a ballasted railway track with under sleeper pads. *Proceedings of the Institution of Mechanical Engineers, Part F: Journal of Rail and Rapid Transit, 225*(3), 299-309.

Standards Australia. (2015). AS 2758.7-2015: Aggregates and rock for engineering purposes, Part 7: Railway ballast. Sydney, New South Wales, Australia.

Steffens, D., & Murray, M. (2005). *Establishing meaningful results from models of railway track dynamic behaviour.* Proceedings of 8th IHHA Conference, Rio de Janeiro, Brazil.